Journal of
Ceramic Science
and Technology

J. Ceram. Sci. Technol., **17** [3] 271-280 (2026)
DOI: 10.4416/JCST2026-00011
available online at: http://www.ceramic-science.com
© 2026 Göller Verlag

Surface Ablation and Mechanical Abrasion of Polymer-Infiltrated Ceramic: Comparative Effects on Surface Microstructure, Roughness, and Adhesive Repair Bond Durability

H.M. Khuthija Khanam*[1], A. Barakat[2], S. Abdul Rahman AlTowayan[3], A. Begum Meer Rownaq Ali[4], T. Almuraikhi[5], A. Alhoumaidan[6]

[1]Department of Restorative and Prosthodontic Department. Dar Al Uloom University, Riyadh.
[2]Department of Restorative and Prosthetic Dental Sciences, College of Dentistry, Dar Al Uloom University, Riyadh, Saudi Arabia.
[3]Assistant Professor in Restorative Dentistry, Department of Conservative Dental Sciences, College of Dentistry, Qassim University, Kingdom of Saudi Arabia.
[4]Riyadh Elm University, Riyadh, Kingdom of Saudi Arabia.
[5]Department of Restorative Dentistry and Prosthodontics, College of Dentistry, Majmaah University, AL-Majmaah 11952, Saudi Arabia.
[6]Department of Prosthodontics, College of Dentistry, Qassim University, Qassim, Saudi Arabia
received June 29, 2026; received in revised form July 13, 2026; accepted July 27, 2026

Abstract

In this study, we compared the effectiveness of airborne-particle abrasion (APA) and Er:YAG laser irradiation (2 W, 4 W) on the surface roughness (R_a), topography, and repair bond strength (RBS) of hybrid ceramic (HBC) repaired via composite bonding using a universal adhesive (UA) with or without a universal primer (UP). A total of 120 HBC discs were embedded in acrylic resin before random allocation into four surface-conditioning groups. Group 1: Control; Group 2: APA (50 μm Al_2O_3); Group 3: Er:YAG laser (2 W); and Group 4: Er:YAG laser (4 W). R_a was measured with a contact profilometer, and SEM was used to assess surface topography. For bond strength testing, specimens were subdivided into Subgroup A (without UP) and Subgroup B (with UP) before UA and composite build-up. Thermocycling was performed, followed by RBS testing using a universal testing machine. Failure modes were assessed stereomicroscopically, and data were analyzed using one-way ANOVA and post hoc Tukey's. Group 1 showed the lowest mean R_a value. The highest R_a scores were recorded in Group 2 (APA). Group 2B (APA+UP+UA) displayed the highest bond strength outcomes. Whereas Group 1A (No conditioning+UA) presented lower RBS. APA and Er:YAG laser irradiation at 4 W, with universal primer application, appeared to demonstrate the most favorable outcomes in terms of R_a and RBS when bonding composite resin to HBC restorations.

Keywords: Hybrid ceramics, VITA Enamic, airborne-particle abrasion, Er:YAG laser, SEM, laser in dentistry, repair bond strength

I. Introduction

Recent advancements in hardware, software, and materials engineering have significantly contributed to the rapid development and enhancement of CAD/CAM technologies [1]. These advancements have equipped dental technicians and clinicians with a diverse array of options for designing dental restorations [2]. The demand for restorative materials that integrate durability, aesthetics, and biocompatibility has markedly increased among restorative practitioners. In this context, hybrid ceramics (HC), also known as resin-matrix ceramic (RMC) materials, have attracted considerable attention in contemporary dentistry [3]. Manufacturers assert that these restorative materials are designed to combine the benefits of ceramics and resin composites, thereby offering a hybrid restorative system with improved machinability, reduced brittleness, and a favorable elastic modulus compared to conventional feldspathic ceramics [1, 4]. Nonetheless, despite these purported advantages, HCs exhibit several limitations, including potential wear of opposing dentition, complex fabrication processes, limited reparability, and inherent brittleness, which complicate their long-term clinical management [5]. Defective restorations are frequently identified in clinical settings, and repair strategies are often preferred over replacement due to their cost-effectiveness and preservation of remaining tooth structure [6].

The adhesive repair of RMC restorations, however, is technically challenging owing to the composite-ceramic interpenetrating network structure of these materials, which renders their surface chemistry distinct from that of either pure ceramics or conventional

* Corresponding author: khuthija@dau.edu.sa

resin composites [7]. Unlike feldspathic porcelains, RMC materials contain a polymer matrix that limits the effectiveness of hydrofluoric acid etching, and unlike pure composites, their ceramic filler content may reduce the efficacy of silane coupling agents alone [8]. This dual-phase nature necessitates careful selection of both surface conditioning and adhesive strategies [9]. Researchers have proposed various surface conditioning methods to enhance the adhesive repair bond strength (RBS) of HC.

Aluminum oxide (Al_2O_3) airborne-particle abrasion (APA) is widely regarded as the gold-standard technique for surface conditioning of RMC before intraoral repair, as it mechanically roughens the surface and increases surface free energy, thereby promoting micromechanical interlocking with repair composites [8, 10]. Nonetheless, there is ongoing debate regarding the optimal particle size and air pressure parameters necessary to achieve the best clinical outcomes [11]. Furthermore, APA is associated with several limitations, including operator health concerns from aerosolized particulates, potential surface degradation due to subsurface crack propagation, and adverse environmental impacts [12, 13]. Therefore, it is justified to evaluate safer and more controlled surface pre-treatment alternatives that minimize harm to both the restorative substrate and the environment.

Lasers have been increasingly employed for the surface pre-treatment of various CAD/CAM dental materials due to their precision, reproducibility, and contactless mode of action, which eliminates the risks of cross-contamination and operator variability associated with particle abrasion [8, 14]. Among available laser systems, the erbium-doped yttrium aluminum garnet (Er:YAG) laser operating at 2 940 nm is particularly advantageous for ablation of inorganic materials, as this wavelength coincides with the peak absorption bands [15 – 17]. In RMC materials, water molecules embedded within the polymer matrix absorb Er:YAG irradiation, generating rapid micro-explosive vaporization that produces a microretentive surface topography without the excessive thermal damage associated with CO_2 or Nd:YAG lasers [16]. This microretentive surface architecture may significantly enhance the mechanical interlocking component of the repair bond. However, laser irradiation can induce internal stresses and potential material damage due to rapid temperature fluctuations during successive heating and cooling cycles, particularly at higher power outputs [18]. Consequently, careful titration of laser operating parameters – particularly power output – is crucial to ensure effective surface roughening without compromising the structural integrity of the underlying restoration. Currently, there is no consensus on the optimal Er:YAG laser parameters for surface pre-treatment to achieve maximum RBS between CAD/CAM hybrid ceramics and repair composites.

In addition to surface pre-treatment, the selection of an appropriate adhesive system is a critical determinant of repair bond durability. The adhesive acts as an intermediary between two chemically and mechanically dissimilar substrates, and its ability to wet and chemically interact with the conditioned RMC surface governs the quality of the bonded interface [19]. Universal adhesives (UA) are simplified, single-bottle bonding systems that incorporate silane, phosphate monomers (MDP), and conventional adhesive components into a single formulation, offering potential advantages of clinical convenience and reduced technique sensitivity [20]. However, the sequential application of a dedicated universal primer (UP) containing silane and MDP before UA may further enhance bonding efficacy by providing more concentrated interfacial chemical interactions with both the ceramic filler and the polymer matrix of the RMC [21]. Studies indicate that the initial bond strength achieved with UA alone is generally comparable to that obtained with a UP-then-UA protocol; however, evidence regarding the durability of this bond following artificial aging – such as thermocycling or prolonged water storage – remains limited and inconsistent, warranting further controlled investigation.

The present study, therefore, aimed to evaluate the effects of different surface conditioning regimens systematically – Er:YAG laser irradiation at 2 W and 4 W, and APA – on surface roughness (R_a) and repair bond strength (RBS) of CAD/CAM hybrid ceramic bonded to composite resin using UA, with or without UP pre-treatment. The null hypotheses proposed were: (1) surface conditioning of hybrid ceramic using Er:YAG laser at different power outputs and APA would produce no statistically significant difference in R_a relative to the unmodified control; and (2) no significant difference in RBS would be observed between UA applied with or without UP pre-treatment, irrespective of surface conditioning method.

II. Materials and Methods

Sample preparation: HBC Vita Enamic (Vita Zahnfabrik, H. Rauter GmbH & Co, Bad Säckingen, Germany) blocks were meticulously sectioned using a cutting machine (Mini CNC XYZ26187, GreatSolutions) equipped with a 0.5-mm-thick diamond cutting disc (Nemofanavaran Pars, Mashhad, Iran) to produce 120 discs, each with a thickness of 2 mm and a diameter of 5 mm. The sample size was determined based on previous published work using the World Health Organization sample size calculation for ANOVA and Post Hoc Tukey. Based on data, a mean RBS of 18.18 MPa and a standard deviation of 0.51 MPa were anticipated. With an absolute effect size of 0.35, a significance level of $\alpha = 0.05$, and a desired statistical power of 0.80, a minimum of 30 specimens per group was calculated, yielding a total sample size of [30 × 4] specimens. All specimens underwent sequential surface polishing with silicon carbide abrasive papers of progressively finer grit sizes (600, 1 000, and 1 200) for 20 seconds under low pressure, with continuous cold-water irrigation. The specimens were subsequently immersed in distilled water and cleaned ultrasonically for 10 minutes using a Sonorex ultrasonic cleaner (Bandelin, Germany). The specimens were embedded in autopolymerizing acrylic resin within standardized molds, ensuring that only the designated treatment surfaces remained exposed. Thereafter, specimens were randomly assigned to four groups based on the surface conditioning method (n = 30) [22].

Group 1: No conditioning No surface conditioners were used in this group.

Group 2: (APA) APA was performed using 50-μm alumina particles (Al_2O_3) delivered via a dental air abrasion unit (Blastmate II™, Ney Dental International, IL, USA) at a standardized air pressure of 80 PSI, using a nozzle-to-surface distance of 5 mm, maintained using a custom-fabricated acrylic positioning jig, and an application duration of 10 seconds per specimen. The nozzle was maintained perpendicular (90 °) to the ceramic surface throughout to ensure uniform particle impingement. Following treatment, specimens were ultrasonically cleaned in distilled water for 5 minutes, rinsed with deionized water, and air-dried with oil-free compressed air for 10 seconds before bonding procedures [23].

Group 3: (Er:YAG laser-2W) An Er:YAG laser (2940 D Plus, DEKA, Italy; DEKA M.E.L.A. Srl, Florence, Italy) was used for HBC surface pre-treatment. The device was operated using an H14-tipped handpiece in non-contact mode, with the tip exit positioned 10 mm from the HBC surface. At this working distance, the irradiated spot diameter was 0.9 mm (spot area = $\pi \times (0.045\ cm)^2 \approx 0.00636\ cm^2$), verified using thermosensitive indicator paper before the experimental procedure. The beam divergence half-angle was estimated as approximately 2.58 °, calculated geometrically as arctan(0.45 mm ÷ 10 mm); this represents a geometric approximation assuming point-source emission at the tip exit, as the manufacturer-specified divergence angle for the H14 tip was not available. The spatial beam profile was multimodal (non-Gaussian), consistent with hollow waveguide delivery in Er:YAG systems operating at 2 940 nm, where conventional silica fiber transmission is not applicable due to high infrared absorption at this wavelength. Laser parameters were as follows: wavelength, 2 940 nm; energy per pulse, 200 mJ; pulse duration, 250 μs (short-pulse mode); repetition rate, 10 Hz; average power, 2 W (verified as internally consistent: 0.200 J × 10 Hz = 2 W); irradiation time per specimen, 20 seconds; total pulses delivered, 200. The single-pulse fluence at the irradiation spot was ≈ 31.45 J/cm². The total energy delivered per specimen was: E_total = 200 mJ × 200 pulses = 40 J. Irradiation was performed using a continuous sweeping motion to ensure uniform surface coverage. Because pulse overlap could not be precisely controlled during freehand sweeping, cumulative fluence per unit area could not be determined with certainty and is therefore not reported; total energy delivered (40 J per specimen) is reported as the reproducible dosimetric parameter. Continuous water spray cooling was applied throughout irradiation at a flow rate of 20 mL/min as measured by timed volumetric collection before the experimental procedure. Surface temperature was monitored using a non-contact infrared thermometer (Fluke 62 MAX; Fluke Corporation, Everett, WA, USA; accuracy: ±1.0 °C). The maximum recorded surface temperature was 42.3 ± 3.1 °C, measured immediately following irradiation [24]. This remained well below the thermal degradation threshold of the resin matrix component of HBC, which has been reported to occur at temperatures exceeding 250 °C, confirming the absence of thermally induced bulk degradation of the substrate. Laser parameters were selected based on previously published protocols for Er:YAG surface pre-treatment of CAD/CAM restorative materials.

Group 4: (Er:YAG laser-4W) The procedure was identical to that of Group 3, with the exception that the power output was raised to 4 W.

R_a assessment: R_a was measured using a contact profilometer (Surftest SJ-201, Mitutoyo, Kawasaki, Japan) with n = 5 samples. Before measurement, the profilometer was calibrated. The standardized settings for the profilometer were as follows: cut-off length of 0.8 mm, tracing length of 4.0 mm, stylus speed of 0.5 mm/s, stylus tip radius of 5 μm, and an applied force of approximately 4 mN. The diamond stylus traversed the specimen surface linearly under constant pressure. Three measurements were taken at distinct locations on each specimen in parallel directions to prevent overlap. The mean R_a value of the three readings was calculated and recorded in micrometers (μm) [25].

Analysis of surface topography For surface characteristic estimation, five discs from each category were coated with gold (Leica, EM ACE200 Sputter Coater; Leica Microsystems, Wetzlar, Germany). Coating was performed under vacuum at 40 mA for 60 s, yielding a gold coating thickness of approximately 10 nm. They were then analyzed employing a scanning electron microscope (SEM) (Hitachi SU1510, Tokyo, Japan) at × 1 000 magnification (n = 5) [26].

Bonding and composite build-up The specimens in each group (n = 20) were divided into two subgroups based on UP application, yielding 10 samples per subgroup (n = 10).

Subgroup A (without UP) In this group, UA was used without UP, followed by a composite build-up.

Subgroup B (with UP) The surfaces in this set were first conditioned with UP (Scotchbond Universal Plus Adhesive; 3M, St. Paul, MN, USA) using a micro applicator, allowed to sit for 60 seconds, and then air-dried. UA (Scotchbond Universal, 3M Deutschland GmbH, Neuss, Germany) was then applied using a microbrush for 20 seconds, followed by air drying until evaporation of solvent, and subsequently light-cured with an LED curing unit (VALO; Ultradent Products Inc., South Jordan, UT, USA) for 10 seconds. A 2 mm increment of composite (GrandioSO A2; VOCO GmbH, Cuxhaven, Germany) was placed within a Tygon tube mold (inner diameter: 3 mm), followed by curing with light for 20 seconds each [27].

Thermal cycling: Each specimen (Groups 1 to 4) was thermally aged using a thermocycler (Vafaei Industrial, Iran) for 10 000 cycles between 5 °C and 55 °C, with 30 s in each bath and a 10-s transfer period. The control samples were not subjected to thermocycling [28, 29].

Evaluation of RBS: RBS testing was performed using a universal testing machine (AGS-X; Shimadzu Corporation, Kyoto, Japan) equipped with a 500-N load cell. Each specimen was individually mounted in a custom-fabricated stainless-steel jig designed to ensure precise axial alignment between the bonded interface and the

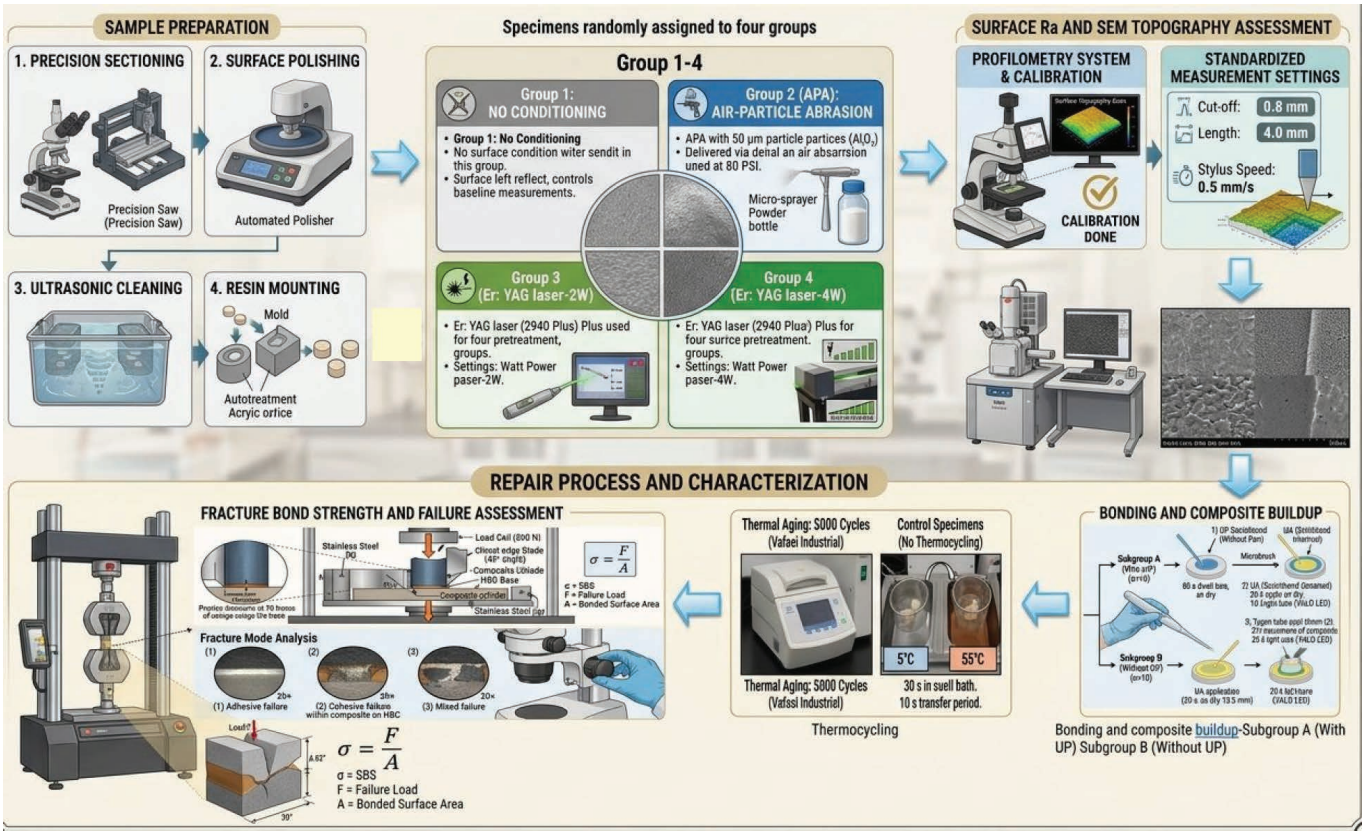

Fig. 1: Methodological workflow.

direction of applied load, thereby minimizing eccentric loading artifacts.

Shear force was applied at the HBC-composite repair interface using a chisel-edge blade (blade angle: 45 °) positioned as close as possible to the bonded interface (≤ 0.5 mm from the base of the composite cylinder) to minimize bending moment contribution to the measured force. Loading was applied at a crosshead speed of 1.0 mm/min under ambient conditions until interfacial failure occurred. The maximum failure load (F) was automatically recorded in newtons. Repair bond strength (RBS, σ) was calculated in megapascals (MPa) using the formula:

$$\sigma = F/A$$

where F is the maximum failure load (N), and A is the bonded surface area (mm²). The bonded surface area was defined by the internal cross-sectional area of the cylindrical Teflon mold used to fabricate the repair composite specimens, with an internal diameter of 3 mm, yielding a bonded area of: [30]

$$A = \pi \times r^2 = \pi \times (1.5)^2 \approx 7.07 \text{ mm}^2$$

Fracture mode analysis. Following mechanical testing, all debonded specimens were examined under a stereomicroscope (Leica Microsystems, Wetzlar, Germany) at 20 × magnification to classify the mode of failure. Fracture modes were categorized as: (1) adhesive failure – complete debonding at the HBC-composite interface with no residual composite on the HBC surface; (2) cohesive failure within composite – cohesive failure within HBC; (3) mixed failure – combination of adhesive and cohesive components. Classification was performed by a single trained examiner blinded to group identity. (Fig. 1)

Statistical analysis: Statistical analysis was conducted using SPSS 29.0 (IBM Corp., Armonk, NY, USA). The normality of the R_a and RBS values was examined using the Kolmogorov-Smirnov and Shapiro-Wilk tests. Statistical evaluation of intergroup differences was conducted using One- way ANOVA with Tukey's post hoc analysis ($p < 0.05$).

III. Results

***R_a* outcomes** Table 1 presents the R_a values of HBC following different surface conditioning protocols. R_a values differed significantly across the evaluated groups ($p < 0.05$). Group 1 showed the lowest mean R_a value (0.36 ± 0.11 µm). Whereas the highest surface R_a scores were recorded in Group 2 (APA) (1.03 ± 0.22 µm). Intergroup comparison analysis revealed that Group 4 (Er:YAG laser-4W) and Group 2 had comparable R_a scores ($p > 0.05$). However, the Group 3 (Er:YAG laser-2W) (0.65 ± 0.14 µm) R_a score was significantly greater than the control, yet significantly lower than Group 2 and Group 4 ($p < 0.05$) (Fig. 2A-2D).

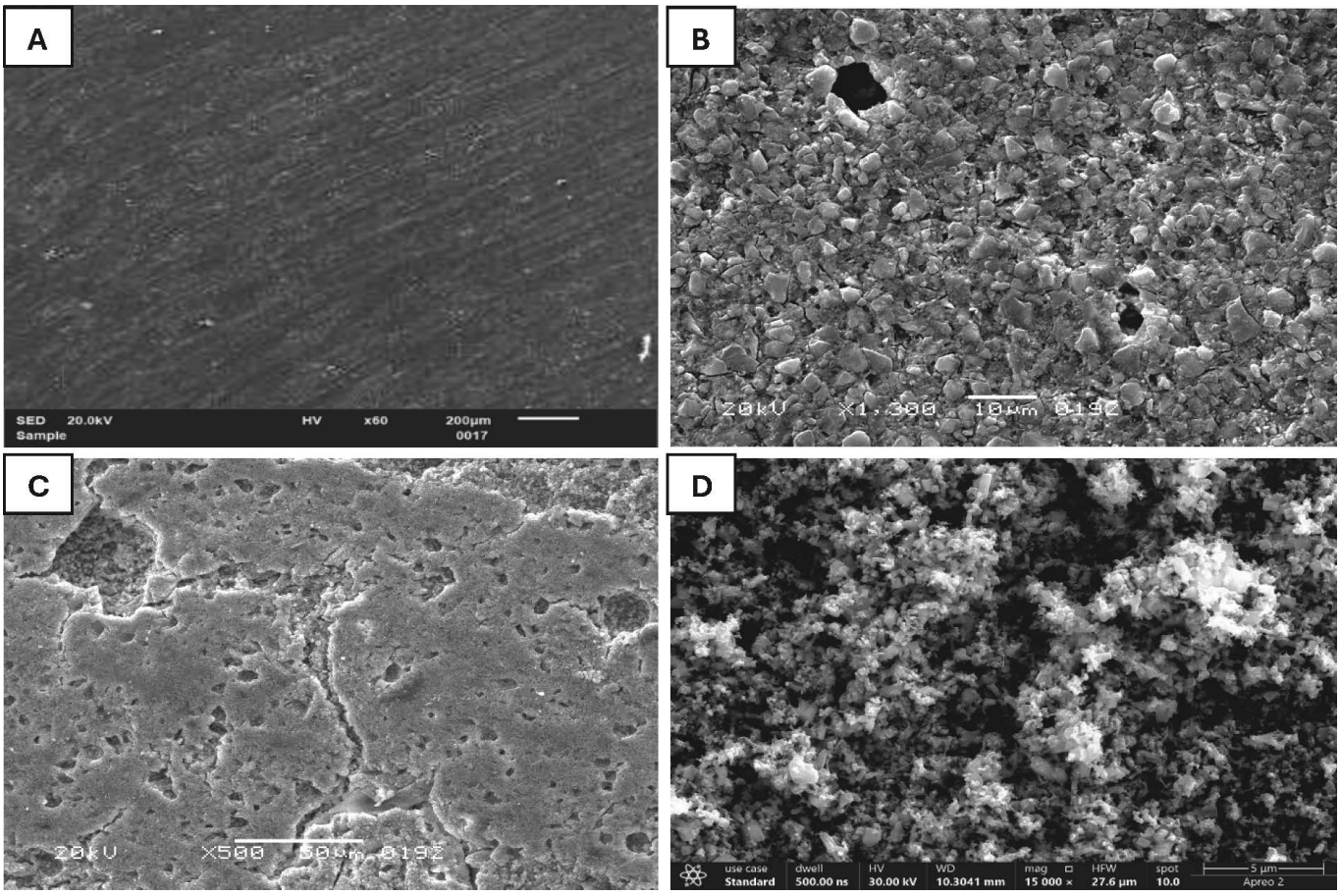

Fig. 2: **A** SEM micrography of the unmodified control hybrid ceramic surface revealed a relatively uniform and smooth topography characterized by parallel polishing striations running diagonally. **B** SEM examination of APA-treated hybrid ceramic surface revealed a markedly altered and heterogeneous surface topography with mechanical disruption characterized by densely distributed irregular granular fragments, angular particle debris, and roughened elevated projections distributed uniformly. Multiple discrete macropores of varying diameter are clearly visible. **C** SEM micrograph of HBC treated with Er:YAG laser @2 W shows overall texture with mild ablation, evidence of thermomechanical material removal manifesting as gently elevated plateau-like regions interspersed with shallow concavities and pit formations of limited depth. **D** SEM image of HBC treated with Er:YAG laser @4 W demonstrates the most extensively ablated and topographically complex surface morphology among all examined groups. The surface demonstrates a densely irregular, highly fragmented architecture characterized by abundant angular crystalline fragments, deeply fractured plateaus, and extensively distributed interparticle voids of varying dimensions. The ablated surface presents a three-dimensional, multi-layered topography with sharply defined elevated fragments of ceramic-polymer matrix material interspersed with deep microporosities and undercut formations.

Table 1: R_a of HBC after the use of different surface pretreatments.

Tested groups	Mean ± SD (µm)	p-value!
Group 1: No conditioning (Control)	0.36 ± 0.11 [a]	
Group 2: APA	1.03 ± 0.22 [c]	
Group 3: Er:YAG laser-2W	0.65± 0.14 [b]	< 0.05
Group 4: Er:YAG laser-4W	1.01 ± 0.20 [c]	

!ANOVA
Airborne particle abrasion (APA), Erbium-doped yttrium aluminum garnet (Er:YAG)
Different superscripts in a column show significant differences, Post Hoc Tukey ($p < 0.05$)

RBS analysis Table 2 presents the RBS of HBC-repaired composite following different surface conditioning regimens, bonded using UA with or without UP pre-treatment. Across all groups, applying UP before UA consistently produced higher RBS values than UA alone, irrespective of the surface conditioning method used ($p < 0.05$). Group 2B (APA + UP + UA) recorded the highest RBS (12.65 ± 0.33 MPa). In contrast, Group 1A (no conditioning + UA) recorded the lowest RBS (6.43 ± 0.28 MPa), with both groups carrying unique superscripts confirming statistically significant differences from all other groups ($p < 0.05$). Intergroup comparison revealed that Group 2B and Group 4B (Er:YAG laser-4W + UP + UA) (12.51 ± 0.12 MPa) demonstrated comparable bond strength performance, with no statistically significant difference observed between them ($p > 0.05$), as indicated by the shared superscript a. Similarly, Group 2A (APA + UA) (10.21 ± 0.42 MPa) and Group 4A (Er:YAG

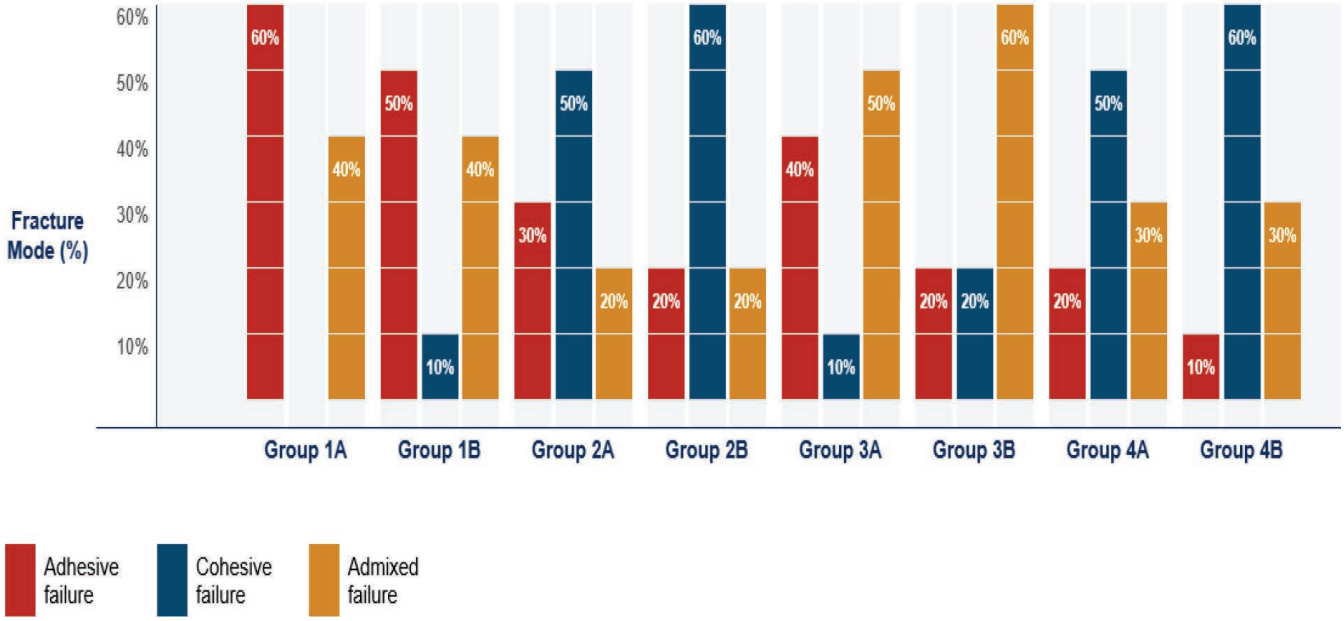

Fig. 3: Grouped bar chart illustrating the percentage distribution of adhesive (red), cohesive (blue), and admixed (amber) fracture modes for each experimental group. Within each group, three adjacent bars represent the three failure categories. Groups 2B and 4B demonstrate dominant cohesive failure (60 %), consistent with the highest recorded repair bond strength values. Groups 1A and 1B show predominantly adhesive failure, corresponding to the lowest bond strength outcomes.

Table 2: RBS of HBC to composite after the use of different surface pretreatment regimes and application of universal adhesive with and without primer.

Bonding and composite buildup	*Mean ± SD (MPa)*	*p-value!*
Group 1A: No conditioning + UA	6.43 ± 0.28^{e}	
Group 1B: No conditioning + UP + UA	7.87 ± 0.14^{f}	
Group 2A: APA+UA	10.21 ± 0.42^{b}	
Group 2B: APA+UP+UA	12.65 ± 0.33^{a}	
Group 3A: Er:YAG laser-2W+UA	8.12 ± 0.48^{c}	*< 0.05*
Group 3B: Er:YAG laser-2W+UP+UA	9.35 ± 0.23^{d}	
Group 4A: Er:YAG laser-4W+UA	10.01 ± 0.51^{b}	
Group 4B: Er:YAG laser-4W+UP+UA	12.51 ± 0.12^{a}	

!ANOVA
Airborne particle abrasion (APA), Erbium-doped yttrium aluminum garnet (Er: YAG), Universal Adhesive (UA), Universal primer (UP)
Different superscripts in a column show significant differences, Post Hoc Tukey ($p < 0.05$)

laser-4W + UA) (10.01 ± 0.51 MPa) exhibited statistically comparable RBS values ($p > 0.05$), both sharing superscript b. Group 3B (Er:YAG laser-2W + UP + UA) (9.35 ± 0.23 MPa) and Group 3A (Er:YAG laser-2W + UA) (8.12 ± 0.48 MPa) demonstrated significantly different RBS values from each other and from all other tested groups ($p < 0.05$). Group 1B (no conditioning + UP + UA) (7.87 ± 0.14 MPa) similarly recorded RBS values that were significantly different from all other groups ($p < 0.05$). These findings indicate that both APA and Er:YAG laser irradiation at 4 W produced superior surface conditioning outcomes compared to 2 W irradiation and no conditioning, with UP pretreatment providing an additional and consistent enhancement of RBS across all surface conditioning subgroups.

Fracture mode assessment: Fig. 3 presents the distribution of fracture patterns among the investigated groups. In the control groups (Groups 1A and 1B), adhesive failure was the predominant mode, accounting for 60 % and 50 % of specimens, respectively, with admixed failure comprising the remaining 40 % in both subgroups and a minor cohesive component (10 %) observed in Group 1B. No purely cohesive failures were recorded in Group 1A, consistent with the lowest bond strength values across all tested groups. Specimens conditioned with APA showed a shift toward cohesive failure, which was the dominant mode in both Group 2A (50 %) and Group 2B (60 %), with a higher proportion in Group 2B reflecting the additional contribution of UP pre-treatment. Similarly, specimens conditioned with Er:YAG laser at 4 W showed predominantly cohesive failure in both Group 4A (50 %) and Group 4B (60 %), accompanied by a notable admixed component (30 % in both subgroups). Specimens irradiated with Er:YAG laser at 2 W exhibited predominantly admixed failure patterns, recorded at 50 % in Group 3A and 60 % in Group 3B, with Group 3A also demonstrating a substantial adhesive failure component (40 %). Across all surface conditioning subgroups, the

application of UP before UA consistently shifted the fracture mode distribution away from adhesive failure and toward cohesive or admixed failure, corroborating the bond strength findings.

IV. Discussion

The present study tested two null hypotheses: first, that surface conditioning of HBC using Er:YAG laser at varying power outputs or APA would produce no statistically significant difference in R_a relative to the unmodified control; and second, that no significant difference in RBS would be observed between UA applied with or without UP pre-treatment, irrespective of the surface conditioning method. The findings of the present study necessitate rejecting both null hypotheses. With respect to the first hypothesis, both APA and Er:YAG laser irradiation at 2 W and 4 W produced significantly higher R_a values than the unmodified control group ($p < 0.05$), confirming that surface conditioning significantly affects the surface roughness of VITA Enamic hybrid ceramic. With respect to the second null hypothesis, the application of UP before UA consistently produced significantly superior RBS across all surface conditioning subgroups ($p < 0.05$), regardless of the pre-treatment method employed, confirming that the adhesive protocol significantly influences composite repair bond strength to HBC.

Studies show that the combination of elevated temperature and pressure during the production of CAD/CAM discs, along with a high monomer conversion, results in a highly polymerized surface that is largely free of carbon-carbon double bonds (C = C) [31]. As a result, surface modification techniques might be required to improve bonding strength. Regarding surface pre-treatment, discs conditioned with APA showed the highest R_a and RBS values. APA enhances the R_a of HBC by mechanically removing material, which creates tiny irregularities, pits, and grooves [32]. This micro-roughened texture increases the surface area available and improves mechanical interlocking with adhesives [8]. Additionally, SEM images support these findings, as HBC discs treated with APA showed roughened surfaces with numerous micropores. On the other hand, Turker *et al.* assessed the bonding of HBC to resin cement and found that APA-treated samples did not differ significantly from the control group [33]. The variation in results can be attributed to APA, indicating that while mild APA use may enhance wettability and micromechanical interlocking, excessive APA could lead to surface damage and compromise material integrity [32,34]. This explains the differing outcomes observed when APA was employed for conditioning hybrid ceramics.

Group 3 (Er:YAG laser-2W) and Group 4 (Er:YAG laser-4W) exhibited significantly higher R_a and RBS values compared with the control. However, Group 4 demonstrated significantly greater R_a and bond strength than Group 3. The primary mechanism of Er:YAG laser interaction with HBC discs is thermomechanical ablation, driven by the high absorption of its 2 940 nm wavelength by water and the inorganic (ceramic) components of the material [35]. However, Shiu and coworkers reported that Er:YAG laser irradiation reduced the bond strength between VITA Enamic and resin cement, attributed to its higher microhardness compared with Lava Ultimate [36]. In the present study, the lower R_a and bond strength observed in Group 3 may be explained by insufficient energy output at 2 W, which was insufficient to achieve the R_a required for effective micromechanical retention, ultimately leading to reduced bond strength. Also, compromised bond integrity may have resulted from the separation of a damaged superficial ceramic layer from the underlying substrate during bond strength testing, thereby contributing to lower RBS values [37,38]. SEM observations further supported these findings, revealing inadequate microdepths of surface porosities at lower power settings, which limited micromechanical retention and consequently reduced bond strength. In contrast, specimens treated at 4 W exhibited higher R_a and bond-strength values, which can be attributed to the more irregular, rougher surface morphology observed in this group. SEM images confirmed the presence of deeper microporosities, increasing the surface area available for resin tag formation and enhancing adhesion to the repair material, thereby improving RBS. Although the 4 W setting effectively increased R_a and bond strength, previous studies suggested that power outputs exceeding 4 W may result in excessive material deterioration and ablation, leading to less porous surfaces that are unsuitable for durable bonding [39].

It was found that groups with UP before the UA application achieved notably higher RBS results than the group with only UA. This could be attributed to the presence of a silane coupling agent in the universal primer. Silanization is well known for improving the bond strength between composite resin and HBC, as the exposed ceramic network on the surface provides a substantial reactive surface for chemical bonding with the silane. Supporting these findings, Günal *et al.* reported that silanization adversely affected the bond strength of resin-matrix ceramics such as Lava Ultimate, whereas VITA Enamic did not show this decrease [40]. Furthermore, Bahadır *et al.* concluded that silane did not enhance bonding in Lava Ultimate but produced improved bond strength in VITA Enamic discs [41]. The authors assume that this inconsistency may be explained by differences in silica content and material microstructure between these hybrid ceramic systems. Unlike UP, the silane-containing UA likely fails to achieve adequate silanization of HBC, which may explain the significantly lower bond strength [42]. Multiple studies have indicated that in Scotchbond Universal, silane performance may be negatively affected by the acidic formulation and coexisting resin components, which supports performing an independent silanization step before adhesion to glass ceramics [43,44].

In this study, the failure modes of the experimental groups were assessed using a stereomicroscope. Adhesive failure predominated in the "A" subgroups (e.g. 60 % in Group 1A, 40 % in Group 3A), whereas cohesive failure was more frequent in the "B" subgroups (60 % in both Groups 2B and 4B). Admixed failure was distributed

variably across groups, peaking at 60 % in Group 3B. Overall, the pattern indicates that subgroup conditioning shifted failure behavior from predominantly adhesive toward cohesive and admixed modes. These findings support the bond-strength results observed in each group and align with the laboratory analysis conducted by Alsunbul *et al.* [45].

This study is subject to several inherent limitations. Firstly, it was conducted in a laboratory setting, which was unable to mimic the intricate conditions of the oral environment fully. The analysis included only a single universal primer and one universal adhesive formulation. Another limitation concerns specimen preparation: samples were sectioned with a slow-speed diamond saw and polished with silicon carbide paper discs, which may not accurately reflect the surface characteristics produced by CAD/CAM milling. Furthermore, atomic force microscopy (AFM) was not utilized for surface characterization; thus, future research incorporating this method is recommended to achieve a more thorough assessment of surface topography.

V. Conclusions

Within the limitations of this *in vitro* study, and considering the constraints inherent to the experimental design, both airborne-particle abrasion and Er:YAG laser irradiation at 4 W combined with universal primer application appeared to demonstrate the most favorable outcomes in terms of surface roughness and repair bond strength for bonding composite resin to Vita Enamic hybrid ceramic restorations. These findings, however, should be interpreted with caution, and further long-term clinical investigations are warranted before definitive recommendations can be made.

Acknowledgments

This research was funded by the General Directorate of Scientific Research & Innovation, Dar Al Uloom University, through the Research Projects Funding Program.

References

[1] Maawadh, A.M., Almohareb, T., Al-Hamdan, R.S., Al Deeb, M., Naseem, M., Alhenaki, A.M., Vohra, F., Abduljabbar, T.: Repair strength and surface topography of lithium disilicate and hybrid resin ceramics with LLLT and photodynamic therapy in comparison to hydrofluoric acid, *J. Appl. Biomater. Funct. Mater.*, **18**, 6938 – 6945, (2020).

[2] Shimoe, S., Peng, T.Y., Otaku, M., Tsumura, N., Iwaguro, S., Satoda, T.: Influence of various airborne-particle abrasion conditions on bonding between zirconia ceramics and an indirect composite resin material, *J. Prosthet. Dent.*, **122**, 491.e1 – 491.e9, (2019).

[3] Samolyuk, G.D., Edmondson, P.D.: First principles study of the stability and thermal conductivity of novel li-be hybrid ceramics, *Acta Mater.*, **215**, 117052, (2021).

[4] David, J., De Matos, M., Rocha, G., Lopes, S., Antonio Queiroz, D., Jiro, L., Nakano, N., Carvalho, N., Ribeiro, R., Barbosa, A.B., Anami, L.C., Bottino, M.A.: Dental ceramics: fabrication methods and aesthetic characterization, *Coatings*, **12**, 1228, (2022).

[5] Duarte, S., Sartori, N., Phark, J.H.: Ceramic-reinforced polymers: CAD/CAM hybrid restorative materials, *Curr. Oral Health Rep.*, **3**, 198 – 202, (2016).

[6] Al-Hamdan, R.S., Almutairi, B., Abduljabbar, T.: Sandblasting, bioactive glass particles, and phthalocyanine activated via low-level laser therapy on the surface roughness and shear bond strength of hybrid ceramics bonded to different cement types, *Photodiagnosis Photodyn. Ther.*, **55**, 104682, (2025).

[7] Campos, F., Almeida, C.S., Rippe, M.P., De Melo, R.M., Valandro, L.F., Bottino, M.A.: Resin bonding to a hybrid ceramic: effects of surface treatments and aging, *Oper. Dent.*, **41**, 171 – 178, (2016).

[8] Shono, N.N., Alkhudhairy, F.: Repair bond strength in hybrid ceramic preconditioned with Ho:YAG laser and toluidine blue, activated by low-level laser therapy, using composites with varying viscosities: an analysis of surface topography and elemental analysis, *Microsc. Res. Tech.*, **88**, 2754 – 2762, (2025).

[9] Ömeroğlu, M.K., Çam, M., Doğruer, I., Kaynar, Z.B.: The effect of different surface treatments and adhesive systems on shear bond strength in universal nanohybrid composite resin repair, *BMC Oral Health*, **25**, 459 – 465, (2025).

[10] Alkhudhairy, F., AlFawaz, Y.F.: Pretreatment of hybrid ceramics using Ho:YAG, low-level laser therapy activated malachite green, and non-thermal plasma on surface roughness, bond strength, and color change, SEM and EDX analysis, *Ceramics*, **7**, 944 – 957, (2024).

[11] Aali, K.A.A.: Repair strength and roughness of resin matrix ceramic pretreated with rose bengal activated low level laser therapy and Er,Cr:YSGG bonded to different viscosity composites, *Photodiagnosis Photodyn. Ther.*, **55**, 104740, (2025).

[12] Tatar, N., Ural, C.: Repair success of two innovative hybrid materials as a function of different surface treatments, *Int. J. Prosthodont.*, **31**, 267 – 270, (2018).

[13] Kanar, Ö., Meşeli, S., Korkut, B., Köken, S., Tağtekin, D., Yanıkoğlu, F.: Assessment of a highly-filled flowable composite for the repair of indirect composites, *J. Oral Sci.*, **66**, 42 – 49, (2024).

[14] Almutairi, B., Al-Hamdan, R.S., Alresayes, S., Alsunbul, H., Alzahrani, K.M., Abduljabbar, T.: Impact of Er;Cr:YSGG laser at different power outputs and hydrofluoric acid on the shear bond strength and color stability of lithium disilicate ceramic and hybrid ceramic, *J. Ceram. Sci. Technol.*, **16**, 93 – 100, (2025).

[15] Vohra, F., Bukhari, I.A., Sheikh, S.A., Naseem, M., Hussain, M.: Photodynamic activation of irrigation (using different laser prototypes) on push out bond strength of fiber posts, *Photodiagnosis Photodyn. Ther.*, **30**, 101716, (2020).

[16] Aljamhan, A.S., Alrefeai, M.H., Alhabdan, A., Alhusseini, S.A., Farooq, I., Vohra, F., Naseem, M., Alkhudhairy, F.: Influence of Er-Cr-YSGG laser and photodynamic therapy on the dentin bond integrity of nano-hydroxyapatite containing resin dentin adhesive: SEM-EDX, micro-raman, micro-tensile, and FTIR evaluation, *Polymers* (Basel), **13**, 1903, (2021).

[17] Alkhudhairy, F., AlKheraif, A., Bin-Shuwaish, M., Al-Johany, S., Naseem, M., Vohra, F.: Effect of er,Cr:YSGG laser and ascorbic acid on the bond strength and microleakage of bleached enamel surface, *Photomed. Laser Surg.*, **36**, 431 – 438, (2018).

[18] Mirhashemi, A.H., Hossaini, S.M.H., Etemadi, A., Kharazifard, M.J., Bahador, A., Soudi, A.: Effect of Er:YAG and Er,Cr:YSGG lasers on ceramic bracket debonding from composite blocks, *Front. Dent.*, **16**, 88 – 95, (2019).

[19] Flury, S., Dulla, F.A., Peutzfeldt, A.: Repair bond strength of resin composite to restorative materials after short- and long-term storage, *Dent. Mater.*, **35**, 1205 – 1213, (2019).

[20] Popescu, M., Maliţa, M., Vorovenci, A., Şteţiu, A.A., Perieanu, V.Ş., Costea, R.C., David, M., Costea, R.M., Şteţiu, M.A.,

Drăguş, A.C., Şerbănescu, C.M., Burlibaşa, A., Eftene, O., Burlibaşa, M.: Wet vs. dry dentin bonding: a systematic review and meta-analysis of adhesive performance and hybrid layer integrity, *Oral*, **5**, 63, (2025).

21 Hilgemberg, B., Siqueira, F.S.F., Cardenas, A.F.M., Ribeiro, J.L., Dávila-Sánchez, A., Sauro, S., Loguercio, A.D., Arrais, C.A.G.: Effect of bonding protocols on the performance of luting agents applied to CAD-CAM composites, *Materials* (Basel), **15**, 6004 – 6010, (2022).

22 Aljamhan, A., Alkhudhairy, F.: Impact of hydrofluoric acid, ytterbium fiber lasers, and hydroxyapatite nanoparticles on surface roughness and bonding strength of resin cement with different viscosities to lithium disilicate glass ceramic: SEM and EDX analysis, *Crystals*, **15**, 661, (2025).

23 Alrabiah, M.A., Alkhudhairy, F.: Effect of sandblasting, tribochemical silica coating, CO_2 laser, and plasma-enhanced chemical vapor deposition on surface characteristics and shear bond strength of 3Y-TZP zirconia, *Crystals*, **16**, 59, (2026).

24 Bayraktar, Y., Demirtağ, Z., Çelik, Ç.: Effect of Er:YAG laser pulse duration on repair bond strength of resin-based and hybrid CAD/CAM restorative materials, J. *Adhes. Sci. Technol.*, **36**, 606 – 619, (2022).

25 Cavalcanti, A.N., Pilecki, P., Foxton, R.M., Watson, T.F., Oliveira, M.T., Gianinni, M., Marchi, G.M.: Evaluation of the surface roughness and morphologic features of Y-TZP ceramics after different surface treatments, *Photomed. Laser Surg.*, **27**, 473 – 479, (2009).

26 AlRefeai, M.H., Alkhudhairy, F.: Glass fiber post pretreated with neodymium-doped yttrium orthovanadate, toluidine blue activated low-level laser therapy, and bioactive glass: an in vitro analysis of SEM, bond strength, and surface roughness, *Crystals*, **15**, 813, (2025).

27 Alrahlah, A., Awad, M.M., Vohra, F., Al-Mudahi, A., Al Jeaidi, Z.A., Elsharawy, M.: Effect of self etching ceramic primer and universal adhesive on bond strength of lithium disilicate ceramic, *J. Adhes. Sci. Technol.*, **31**, 2611 – 2619, (2017).

28 Vohra, F., Labban, N., Al-Hussaini, A., Al-Jarboua, M., Zawawi, R., Alrahlah, A., Naseem, M.: Influence of Er;Cr:YSGG laser on shear bond strength and color stability of lithium disilicate ceramics: an in vitro study, *Photobiomodulation Photomed. Laser Surg.*, **37**, 483 – 488, (2019).

29 Albaker, A.M., Al Deeb, L., Alhenaki, A.M., Aldeeb, M., Al Ahdal, K., Abduljabbar, T., Vohra, F.: Bonding integrity and compressive strength of re-bonded, surface conditioned and Er,Cr:YSGG laser treated lithium disilicate ceramics, *J. Appl. Biomater. Funct. Mater.*, **18**, 2280800020910954, (2020).

30 Bello, Y.D., Di Domenico, M.B., Magro, L.D., Lise, M.W., Corazza, P.H.: Bond strength between composite repair and polymer-infiltrated ceramic-network material: effect of different surface treatments, *J. Esthet. Restor. Dent.*, **31**, 275 – 279, (2019).

31 Stawarczyk, B., Basler, T., Ender, A., Roos, M., Özcan, M., Hämmerle, C.: Effect of surface conditioning with airborne-particle abrasion on the tensile strength of polymeric CAD/CAM crowns luted with self-adhesive and conventional resin cements, *J. Prosthet. Dent.*, **107**, 94 – 101, (2012).

32 Aljamhan, A., Alkhudhairy, F.: Effect of pre-treatment techniques Nd:YLF laser, nano-HAp particles on surface roughness and repair bond strength of different-viscosity composite bonded to hybrid ceramics, *J. Ceram. Sci. Technol.*, **16**, 263 – 268, (2025).

33 Türker, N., Büyükkaplan, U.Ş., Başar, E.K., Özarslan, M.M.: The effects of different surface treatments on the shear bond strengths of two dual-cure resin cements to CAD/CAM restorative materials, *J. Adv. Prosthodont.*, **12**, 189 – 196, (2020).

34 Alkhudhairy, F., Naseem, M., Ahmad, Z.H., Alnooh, A.N., Vohra, F.: Efficacy of phototherapy with different conventional surface treatments on adhesive quality of lithium disilicate ceramics, *Photodiagnosis Photodyn. Ther.*, **25**, 292 – 295, (2019).

35 Almutairi, B., Al-Qahtani, A.S., Shabbir, T., Leemani, M.J., Unar, J., Manzar, N., Abduljabbar, T.: A surface topographical analysis of lithium disilicate ceramics pretreated with rose bengal, Er:YAG laser, and ceramic primer on bond integrity, surface roughness, and bond failure to composite resin, *Sci. Adv. Mater.*, **16**, 800 – 806, (2024).

36 Usta Kutlu, İ., Yerliyurt, K.: The impact of various surface treatments and Er-YAG laser irradiation on the bond strength of resin matrix CAD/CAM ceramics to resin cement, *Lasers Med. Sci.*, **40**, 201 – 207, (2025).

37 Özdemir, H., Aladağ, L.İ.: Effect of different surface treatments on bond strength of different resin cements to lithium disilicate glass ceramic: an in vitro study, *Biotechnol. Biotechnol. Equip.*, **31**, 815 – 820, (2017).

38 Yilmaz-Savas, T., Demir, N., Ozturk, A.N., Kilic, H.S.: Effect of different surface treatments on the bond strength of lithium disilicate ceramic to the zirconia core, *Photomed. Laser Surg.*, **34**, 236 – 243, (2016).

39 Hou, Y., Shen, R., Chen, L., Chen, Y., Jiang, Y., Li, J.M., Gao, J.: Shear bond strength of different CAD/CAM ceramics: acid vs Er:YAG laser etching, *Photomed. Laser Surg.*, **36**, 614 – 620, (2018).

40 Günal-Abduljalil, B., Önöral, Ö., Ongun, S.: Micro-shear bond strengths of resin-matrix ceramics subjected to different surface conditioning strategies with or without coupling agent application, *J. Adv. Prosthodont.*, **13**, 180 – 190, (2021).

41 Bahadir, H.S., Bayraktar, Y.: Evaluation of the repair capacities and color stabilities of a resin nanoceramic and hybrid CAD/CAM blocks, *J. Adv. Prosthodont.*, **12**, 140 – 149, (2020).

42 Hoseinifar, R., Shadman, N., Mirrashidi, F., Gholami, S.: The effect of silane-containing universal adhesives on the immediate and delayed bond strength of repaired composite restorations, *Dent. Res. J.* (Isfahan), **18**, 87, (2021).

43 Elsayed, A., Younes, F., Lehmann, F., Kern, M.: Tensile bond strength of so-called universal primers and universal multimode adhesives to zirconia and lithium disilicate ceramics, *J. Adhes. Dent.*, **19**, 221 – 228, (2017).

44 Yao, C., Yang, H., Yu, J., Zhang, L., Zhu, Y., Huang, C.: High bond durability of universal adhesives on glass ceramics facilitated by silane pretreatment, *Oper. Dent.*, **43**, 602 – 612, (2018).

45 Alsunbul, H., Almutairi, B., Aljanakh, M., Abduljabbar, T.: Hybrid ceramic repair strength, surface roughness, and bond failure, using methylene blue-activated low-level laser therapy, carbon dioxide, and Ti:Al_2O_3 laser, *Photodiagnosis Photodyn. Ther.*, **43**, 103693, (2023).